ISSN 0208-7774 TRIBOLOGIA 1/2024 p. 89–98
DOI: 10.5604/01.3001.0054.4658

Leszek ŁATKA[*], Karolina PŁATEK[**], Mirosław SZALA[***], Piotr KORUBA[****], Paweł SOKOŁOWSKI[*****], Jacek REINER[******]

COMPARATIVE STUDY OF METAL-MINERAL ABRASIVE WEAR RESISTANCE OF HARDFACING LAYERS PRODUCED THROUGH DIFFERENT METHODS

BADANIA PORÓWNAWCZE ODPORNOŚCI NA ZUŻYCIE ŚCIERNE TYPU METAL–MINERAŁ WARSTW NAPAWANYCH RÓŻNYMI METODAMI

Key words: hardfacing, FCAW, PTAW, LMDW, abrasive wear resistance, high energy density methods, flux-cored wire.

Abstract: This article presents a comparison of the results of metal-mineral abrasion resistance investigations of hardfacing layers produced through different welding methods: (i) arc, (ii) plasma, and (iii) laser. Flux-cored wire with a metallic core (SK600-G) was used as a feedstock material. The work investigated the influence of basic hardfacing parameters on the geometry, microstructure, and correctness of making single beads . Then, full layers were made with the parameters selected for each method and abrasion resistance tests were carried out in accordance with the ASTM G65 standard. The obtained test results were analyzed for mechanical properties and microstructure of the produced padding welds. On the basis of the tests and analysis of the results, it was found that the use of methods with high energy density has a positive effect on the reduction in the coefficient of the share of the base material in the padding weld, while increasing the hardness. Comparative analysis of the resistance to metal-mineral abrasive wear showed that the resistance was approx. 25% higher for plasma layers and approx. 35% for laser layers, compared to electric arc-deposited layers.

Słowa kluczowe: napawanie, FCAW, PTAW, LMDW, odporność na zużycie ścierne, metody o wysokiej gęstości energii, drut proszkowy.

Streszczenie: W artykule przedstawiono porównanie odporności na zużycie ścierne typu metal–minerał warstw napawanych różnymi metodami spawalniczymi: (i) łukowo, (ii) plazmowo oraz (iii) laserowo. Jako materiał dodatkowy zastosowano drut proszkowy z rdzeniem metalicznym (SK600-G). W pracy badano wpływ podstawowych parametrów napawania na geometrię, mikrostrukturę oraz poprawność wykonania pojedynczych ściegów. Następnie wykonano pełne warstwy wybranymi parametrami dla każdej z metod i przeprowadzono badania odporności na zużycie ścierne, zgodnie z normą ASTM G65. Uzyskane wyniki badań analizowano w kontekście własności mechanicznych oraz budowy mikrostrukturalnej wytworzonych napoin. Na podstawie analiz wyników badań stwierdzono, że zastosowanie metod o wysokiej gęstości energii korzystnie wpływa na redukcję współczynnika udziału materiału podłoża w napoinie, przy jednoczesnym wzroście twardości. Porównując odporność na zużycie ścierne typu metal–minerał zaobserwowano zmniejszone zużycie o ok. 25% dla napoin plazmowych oraz o ok. 35% dla napoin laserowych w porównaniu do napoin wykonanych metodą łukową.

[*] ORCID: 0000-0002-5236-5349. Wrocław University of Science and Technology, Department of Metal Forming, Welding and Metrology, Faculty of Mechanical Engineering, 5 Łukasiewicza St., 50371 Wrocław, Poland.
[**] Wrocław University of Science and Technology, Department of Metal Forming, Welding and Metrology, Faculty of Mechanical Engineering, 5 Łukasiewicza St., 50371 Wrocław, Poland.
[***] ORCID: 0000-0003-1059-8854. Lublin University of Technology, Department of Materials Engineering, Faculty of Mechanical Engineering, 36D Nadbystrzycka St., 20618 Lublin, Poland.
[****] ORCID: 0000-0001-6270-4167. Wrocław University of Science and Technology, Department of Laser Technology, Automation and Production Engineering, Faculty of Mechanical Engineering, 5 Łukasiewicza St., 50371 Wrocław, Poland.
[*****] ORCID: 0000-0003-2425-2643. Wrocław University of Science and Technology, Department of Metal Forming, Welding and Metrology, Faculty of Mechanical Engineering, 5 Łukasiewicza St., 50371 Wrocław, Poland.
[******] ORCID: 0000-0003-1662-9762. Wrocław University of Science and Technology, Department of Laser Technology, Automation and Production Engineering, Faculty of Mechanical Engineering, 5 Łukasiewicza St., 50371 Wrocław, Poland.

INTRODUCTION

To maintain high operational performance and extend components durability, enhancing the abrasion resistance of its outer layer is essential. However, using high abrasion-resistant materials for the entire component is frequently economically and technologically impractical due to the associated high costs and processing challenges. Therefore, the improvement of surface properties alone often proves sufficient to attain the required characteristics **[L. 1, 2]**. The surface tribological properties can be improved by depositing an outer layer of a material with superior properties compared to those of the base material. Welding techniques can be employed for this purpose **[L. 3–5]**. This process is referred to as hardfacing, and the deposited layers are called hardfacing layers. Nearly all welding processes can be successfully applied for hardfacing. Often referred as a more economical alternative to shielded metal arc welding (SMAW), flux-cored arc welding (FCAW) is one of the most common ones, especially for restoration of damaged parts **[L. 6, 7]**. In FCAW, the filler material has the form of a wire tube filled with metal powder and flux, whose chemical composition is often similar to the shielding cover of electrodes used in SMAW. The form of the filler material provides a great variety of possible chemical compositions and high deposition rates, since feeding can be easily automated **[L. 8–10]**.

The term 'High Energy Density' (HED) welding refers to all welding processes capable of focusing energy within a confined area. This capability, along with high energy sources, provides extremely high energy density. Consequently, both the fusion and heat-affected zones exhibit relatively narrow dimensions, mitigating the adverse effects of chemical and thermal distortions. Only a few welding methods have this capability, with plasma, laser, and electron beam welding among the most commonly employed ones.

Plasma transferred arc welding (PTAW) originates from gas tungsten arc welding (GTAW). However, in contrary to GTAW, due to higher concentration of energy, PTAW provides lower dilution ratio and narrower heat affected zone (HAZ) **[L. 11]**. Both these properties are highly desired in hardfacing. PTAW process is already widely deployed in the manufacturing industry and its most common applications include corrosion, abrasion, and high-temperature resistant layers for marine, mining, agricultural, and energy industries **[L. 12–14]**. Laser and electron beam welding (denoted as LBW and EBW, respectively) are superior to other welding techniques in creating narrow, high depth weld joints with high speeds **[L. 15, 16]**. However, thanks to lower cost and less stringent requirements as regards working conditions than EBW, LBW is often mentioned as the main candidate for manufacturing high-performance components for automotive, aerospace, nuclear, and additive manufacturing industries **[L. 17–19]**. The applications of laser metal deposition welding (LMDW) are widely described in **[L. 20–22]**.

In both plasma and laser welding, the majority of research concentrates on the utilization of a filler material in the powder form **[L. 23, 24]**. There is a scarcity of publications that describe the application of a filler material in the wire form. In **[L. 25]** authors described the impact of PTAW parameters on the properties of austenitic steel coating on C45 steel. PTAW cladding with multiple wire feeding was used for deposition of high-entropy alloys what was described in **[L. 26]**. Kripalani et. al. **[L. 27]** investigated various methods of deposition Nitinol wire on AISI 304 plate, including plasma welding and laser as heat source. All the above-mentioned articles focus on a filler material in the form of a solid wire. However, recently, there has been a growing interest in using cored wires for laser hardfacing. Zhao et. al. examined the possibility of laser wire deposition of Ni/WC and Fe/WC composites, achieving highly promising results **[L. 28–30]**. In this study, the filler material had the form of a tubular cored wire with a diameter of 1.6 mm. In **[L. 31]**, Wang et. al. described fabrication and wear behavior of (TiB2 + TiB + TiC)/Ti coating. The use of wires instead of powders brings several advantages, e.g. full use of materials usage and ability of deposition beads in different welding positions **[L. 32]**. Additionally, due to smaller specific surface, a wire might contribute to reducing chemical reactivity. This property is especially beneficial in the case of materials with high oxidation tendency, such as titanium and aluminum alloys.

In this article, we examined and compared abrasive wear resistance of Fe-based hardfacing layers deposited from a flux-cored wire using different welding techniques what, to the authors' best' knowledge, have not yet been described. The conventional FCAW method was compared with HED methods, namely PTAW and LMDW. As

a filler material, Böhler SK 600-G wire was used. Due to its excellent abrasive wear resistance, this material has already found plenty of applications in the manufacturing industry, especially in the metallurgical and mining sectors **[L. 33]**. We investigated the influence of the basic hardfacing parameters on the geometry and microstructure of the deposited beads, to select the sets of parameters providing the best outcome. The chosen conditions were used for the deposition of hardfacing layers, which were further tested in terms of the abrasion wear resistance.

MATERIALS AND METHODS

Filler material, Böhler SK 600-G, in standard of DIN 8555: MF 6-GF-60-GP, had the form of a cored wire with a diameter of 1.2 mm. As a base material, structural steel S235JR in the form of a 150 x 100 mm and 10 mm thick plate was used. Chemical composition of the filler material in accordance with the EN 14700:2023-04 standard **[L. 34]** is presented in Table 1, while chemical composition of the base material in accordance with the EN 10025 standard **[L. 35]** is shown in **Table 2**.

Table 1. Chemical composition (in wt.%) of the filler material in accordance with the EN 14700:2023-04 standard [L. 34]
Tabela 1. Skład chemiczny (w% wag.) materiału dodatkowego zgodnie z normą EN 14700:2023-04 **[L. 34]**

C	Mn	Si	Cr	Mo	Ti	Fe
0.52	1.5	1.2	5.9	0.8	0.05	Balance

Table 2. Chemical composition (in wt.%) of the base material in accordance with the EN 10025 standard [L. 35]
Tabela 2. Skład chemiczny (w% wag.) materiału podstawowego zgodnie z normą EN 10025 **[L. 35]**

C	Mn	P	S	Cu	N	Fe
0.17	1.4	0.0355	0.035	0.55	0.012	Balance

FCAW hardfacing was performed using qa Lincoln Electric POWERTEC 505S power source. As shielding gas, a mixture of Ar with the addition of 2 vol.% O2 was used (M13-ArO-2 in accordance with **[L. 37]**). For PTAW welding, a Castolin EuTronic® GAP 3511 DC Synergic source was applied. During the process, the welding area was shielded by 100% Ar (I1). LMDW hardfaces were made using LaserLine HPDL LDF 4000-30. Similarly to the PTAW process, I1 was used as shielding gas.

The ranges of process parameters were specified based on the preliminary tests. As variables, welding speed and electric current were chosen in the case of FCAW and PTAW hardfacing, while for LMDW, the variables were welding speed and laser power. All possible combinations of parameter values were tested and in total, 9 samples per each method were made. The values of the variable parameters are presented in **Table 3**.

Table 3. Hardfacing variable parameters
Tabela 3. Zmienne parametry napawania

FCAW	*Welding current [A]*	140	175	210
	Welding speed [mm/s]	8.0	10.0	12.0
PTAW	*Welding current [A]*	100	115	130
	Welding speed [mm/s]	1.8	2.0	2.2
LMDW	*Laser power [kW]*	2.0	2.5	3.0
	Welding speed [mm/s]	5.0	7.5	10.0

After deposition, the beads underwent visual testing (VT), as well as macroscopic observations. The VT was performed right after deposition with an unaided eye with the aim to detect surface defects. To detect potential welding imperfections (lack of fusion (401), excess weld metal (502), incorrect weld toe (505), intermittent undercut (5012), according to ISO 6520-1 standard **[L. 37]**), the macroscopic observations were conducted on samples cross-section using a Keyence VHX6000 digital microscope. Subsequently, the dilution ratio was determined (**Figure 1**) using the same

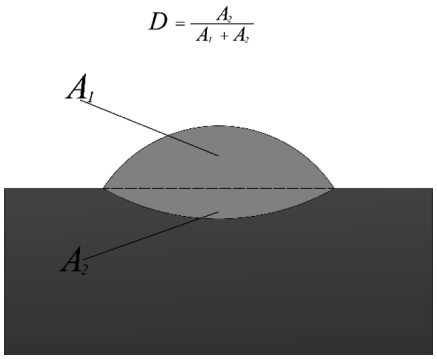

Fig. 1. Scheme presenting the dilution ratio determination method
Rys. 1. Schemat przedstawiający metodę wyznaczania współczynnika wymieszania

apparatus. The microstructure was analyzed with a VEGA3 Tescan scanning electron microscope (SEM). Prior to examination, samples were polished and etched using aqua regia. Subsequently, hardness of the deposited layers was measured using Vickers hardness method in accordance with the ISO 9015-2 standard **[L. 38]**. The test force was equal to 9.81 N (HV1). For each sample, 12 measurements were taken at the distance of 1 mm from welds face, with a constant interval of 0.5 mm between each measurement. The details of the test conditions are presented in **Figure 2.** The distance between each measurement was adapted to the width of the beads.

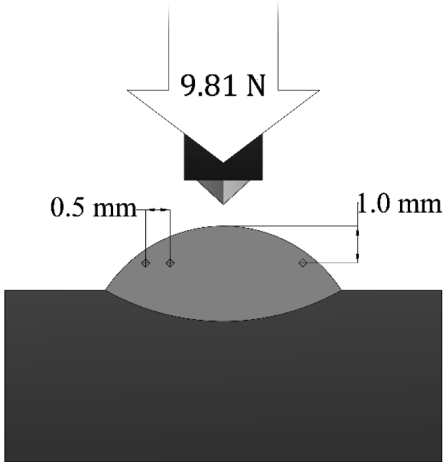

Fig. 2. Scheme presenting the hardness measurement method
Rys. 2. Schemat przedstawiający metodę pomiaru twardości

Based on the results of the above-described examinations, a set of optimal parameters was selected for each method. They were subsequently applied for the deposition of a hardfacing layer and used for functional characteristics examination. After deposition, hardfacing layers were grinded and samples with dimensions of 29x29 mm were obtained (**Figure 3**). The abrasion wear resistance of the hardfacing layers was examined in accordance with the ASTM G65 standard (procedure D), using the rubber wheel apparatus **[L. 39]**. Corundum sand with an average particle size of 0.18 mm was used as the abrasive. The sand was fed at a rate of 300 g/min. The total number of revolutions conducted was 6,000, with the rubber wheel operating at a speed of 200 rpm. During the test, the specimen was subjected to a load of 45 N. The test procedure is illustrated in Figure 4. Abrasion wear resistance of hardfacing layers was determined through value of mass loss. Additionally, surface roughness and wear trace area were measured.

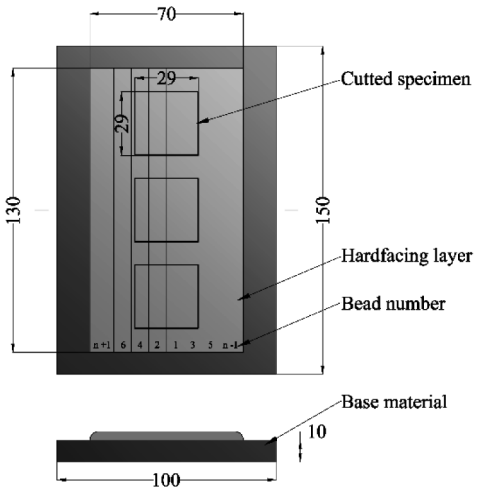

Fig. 3. Sample preparation scheme
Rys. 3. Schemat przygotowania próbek

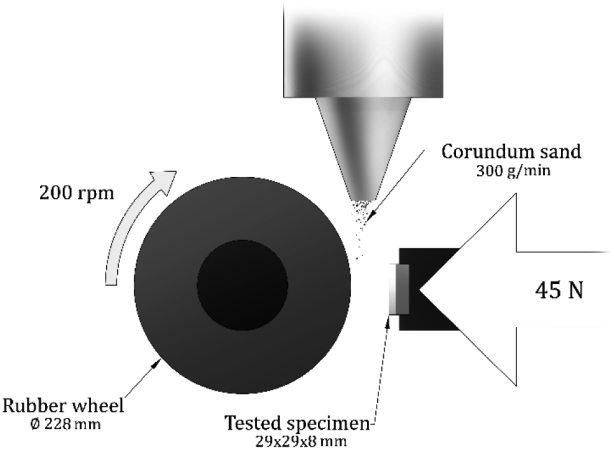

Fig. 4. Abrasive wear test scheme
Rys. 4. Schemat badania odporności na zużycie ścierne

RESULTS AND DISCUSSION

No significant surface defects were noticed during the VT examination. On the other hand, macroscopic observations (**Figure 5**) revealed presence of welding imperfections, namely discontinuities (visible in **Figure 5a**). Defects occurred mainly in beads deposited with lowest welding energy, resulting from i) low value of electric current or laser power; or ii) high welding speed. The largest number of imperfections was observed for beads deposited using the LMDW method, while for the PTAW method, this number was the lowest. This phenomenon is a result of high sensitivity to disruption and narrow processing window, characteristic for this method.

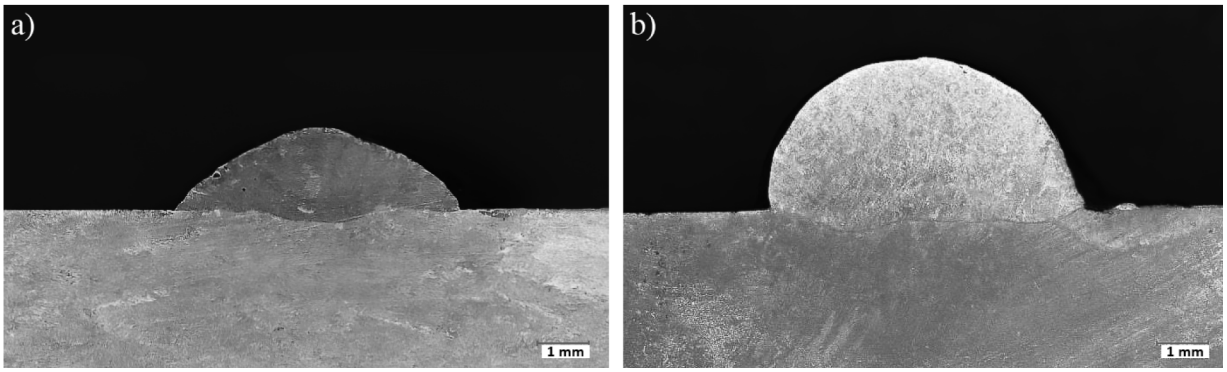

Fig. 5. Macroscopic observations of sample beads deposited using: a) LMDW method: visible discontinuities resulting from high welding speed, porosity, b) PTAW method: low dilution ratio and no significant welding imperfections

Rys. 5. Obserwacje makroskopowe przykładowych napoin wykonanych metodą: a) LMDW: widoczne niezgodności typu przyklejenia wynikające ze zbyt wysokiej prędkości napawania, b) PTAW: niska wartość współczynnika wymieszania, brak znaczących niezgodności spawalniczych

The values of the dilution ratio varied from 12.9% to 26.2% for FCAW method, from 9.5% to 18.9% for PTAW-deposited beads, and from 6.4% to 14.2% for LMDW-deposited beads. Regardless of the method used, the lowest value of the dilution ratio was measured for beads deposited at highest welding speed.

Despite using filler materials of uniform chemical composition, hardness of the deposited beads varied significantly between each method. The lowest average hardness was measured for specimens deposited using the FCAW method (ranging from 539 to 588 HV1), while for LMDW the range of hardness was 657–731 HV1. The average value of hardness measured for PTAW-deposited samples ranged from 592 to 678 HV1. To compare, the value of hardness declared by the manufacturer was 59 HRC. Only a few studies on materials of similar chemical composition were found and most of them reported a slightly lower value of hardness in comparison with that obtained for both the PTAW and LMDW hardfaces **[L. 40]**.

Based on the results obtained, a set of optimal parameters was selected for each method. The choice was determined by i) the presence of welding imperfections; ii) the value of dilution ratio; and iii) the hardness of the hardfacing layer. Selected welding parameters are presented in **Table 4**.

The microstructures of the beads deposited using the above-listed parameters are shown in **Figure 6**. All deposited samples exhibit a similar fully martensitic microstructure. In the case of the LMDW-deposited bead, its microstructure demonstrates a high degree of density and homogeneity. The grains within this microstructure are smaller, and directional orientation of the structure is barely discernible, particularly when compared to the PTAW sample. Furthermore, unlike the FCAW- and PTAW-deposited samples, no porosity was observed in the microstructure of the specimens deposited using the LMDW method. The differences in both hardness value and microstructure arise from different cooling conditions. According to the literature **[L. 41]**, in the case of martensitic structure, higher cooling rates result in higher hardness and finer structure. This assumption corresponds with the outcome of the conducted examinations. Moreover, the selected beads have the fewest welding imperfections, and the dilution ratio remained at relatively low level (19.4% for FCAW, 13.1% for PTAW, and 11.4% for LMDW-deposited beads). The hardness of the selected beads was equal to 574 ± 54 HV1 for FCAW; 678 ± 62 HV1 for PTAW; and 729 ± 49 HV1 for LMDW method. The LMDW sample also has the lowest area of the heat affected zone, which is favorable.

Table 4. Parameters chosen for hardfacing layer deposition

Tabela 4. Parametry wybrane do napawania warstw

FCAW	*Welding current [A]*	210
	Welding speed [mm/s]	10.0
PTAW	*Welding current [A]*	115
	Welding speed [mm/s]	2.0
LMDW	*Laser power [kW]*	2.0
	Welding speed [mm/s]	7.5

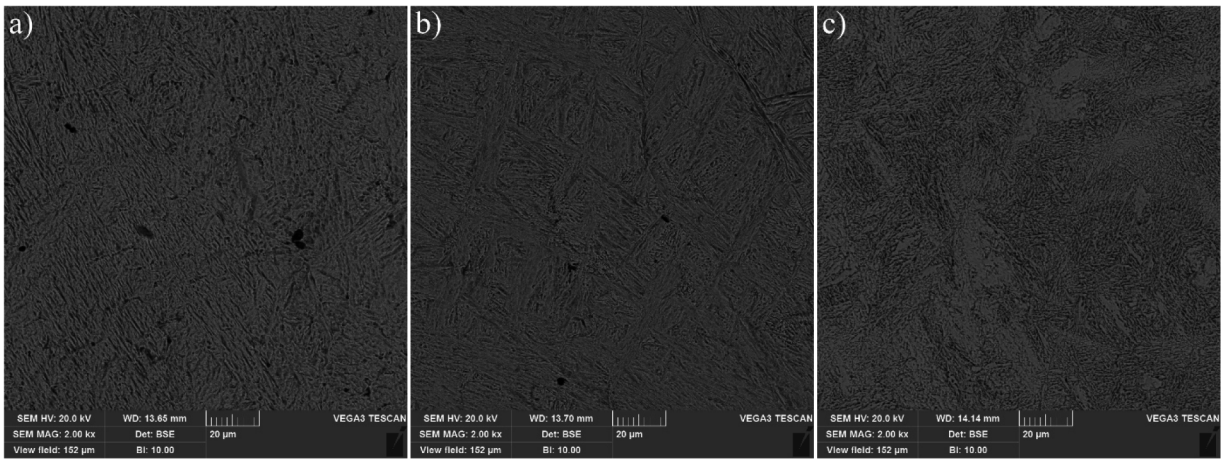

Fig. 6. Microstructure of beads deposited under chosen conditions using: a) FCAW, b) PTAW, c) LMDW method
Rys. 6. Mikrostruktura ściegów wykonanych przy wybranych parametrach metodą: a) FCAW, b) PTAW, c) LMDW

As a result of the abrasive wear test, the value of the average mass loss was determined (**Fig. 7**). The mass loss measured for samples deposited using the FCAW method was the highest reaching 458.24 ± 41.33 mg. Both PTAW and LMDW hardfaces showed a significantly better abrasion wear resistance with a mass loss of 323.52 ± 29.85 and 235.61 ± 22.42 mg. Wear area measurements confirmed the previously described lower abrasion wear resistance of hardfacing layers deposited by FCAW, in comparison with those deposited by both PTAW and LMDW. Furthermore, the surface roughness Sa of the FCAW-deposited sample was nearly twice that of PTAW and LMDW-deposited samples. Both characteristics are detailed in **Table 5**.

SEM observations of the wear trace area (**Figure 8**) enabled the detection of mainly two mechanisms responsible for material loss: abrasion and micro-pitting. Transverse grooving predominantly manifested in the FCAW-deposited samples, as illustrated in **Figure 9a**. Furthermore, the occurrence of a loose material can be attributed to micro-pitting **[L. 42]**. Continuous grooves, aligned parallel to the rotation direction, are discernible in both **Figure 9b** and **Figure 9c**, signifying a high degree of material homogeneity. Conversely, in the case of PTAW-deposited coatings, micro-pitting exhibited significantly greater intensity. Additionally, the presence of ledges along certain wear tracks suggests that a negligible amount of plastic deformation took place during the abrasion process. Even though such phenomenon is not particularly expected due to high hardness of the material, the observations correspond with findings described in **[L. 43]**. Similar behavior was also noted in the case of Hardox 500 in **[L. 44]**.

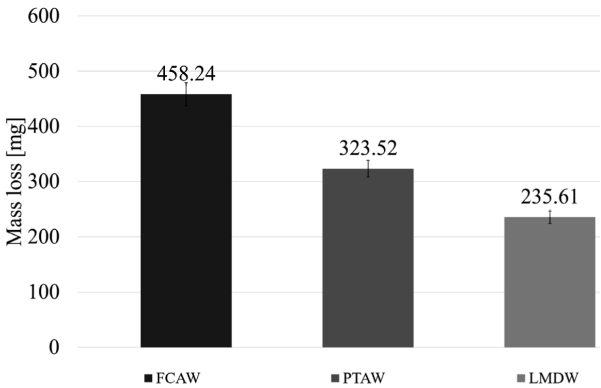

Fig. 7. Average mass loss after abrasive wear test
Rys. 7. Średni ubytek masowy na skutek testu odporności na zużycie ścierne

Table 5. Values of wear trace area and surface roughness
Tabela 5. Wartości śladu wytarcia oraz chropowatości powierzchni w jego obszarze

	FCAW	PTAW	LMDW
Wear trace area [mm²]	37.53 ± 3.31	19.24 ± 1.72	16.43 ± 1.44
Surface roughness Sa [µm]	55.83 ± 4.47	34.39 ± 2.95	29.51 ± 2.43

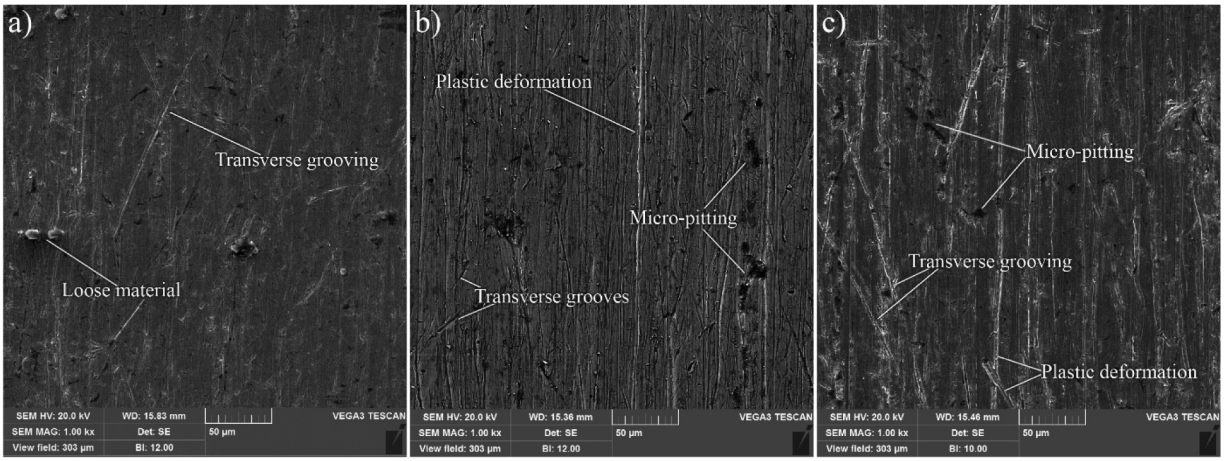

Fig. 8. Wear traces depicted SEM: a) FCAW, b) PTAW, c) LMDW
Rys. 8. Powierzchnia śladu wytarcia obserwowana przy pomocy SEM: a) FCAW, b) PTAW, c) LMDW

CONCLUSIONS

In the presented research, the possibility of using cored wire as filler material for high energy density hardfacing methods was examined and proved. As a result of the study, the following conclusions were formulated:

1. The use of high energy density methods, such as PTAW or LMDW, results in higher hardness and lower dilution ratio. The hardness of deposited hardfacing layers varied from 574 ± 57HV1 for samples deposited using FCAW, to 729 ± 49 HV1 for LMDW. The discrepancy results from lower dilution ratio, as well as higher cooling rates of LMDW-deposited samples, which resulted in finer microstructure and lower porosity percentage.
2. Regardless of the method, higher welding speed results in lower dilution ratio and higher hardness. However, this paired up with low value of electric current / laser energy, leads to presence of welding imperfections (namely discontinuities).
3. Microstructure observations showed that hardfaces deposited using HED methods present much denser and more homogenous martensitic structure in comparison with conventional methods.
4. Abrasion wear resistance of samples deposited using LMDW method was almost twice that of FCAW. Moreover, surface roughness of conventionally made layers was 55.93 µm, while for PTAW and LMDW surface roughness Sa was equal to 34.39 and 29.51 µm respectively, which is due to better material homogeneity.

HED methods provide enhanced abrasion wear resistance of deposited hardfacing layer, directly contributing to the extension of component durability. However, certain drawbacks must be acknowledged. It is necessary to emphasize that HED methods exhibit higher sensitivity to disruption and narrower processing window in comparison with conventional methods, which can lead to the occurrence of welding imperfections. Additionally, the equipment costs associated with HED methods are relatively substantial. Given these considerations, further research into the application of HED methods, such as PTAW and LMDW, in lieu of FCAW is needed. Moreover, evaluations of the corrosion and erosion resistance of the discussed hardfaces should be conducted. Lastly, the possibility of employing cermet cored wire requires further investigation.

REFERENCES

1. Balaguru S., Gupta M.: Hardfacing studies of Ni alloys: a critical review, Journal of Materials Research and Technology, vol. 10, p. 12101242, 1, 2021.
2. Fouad Y., Marouani H.: Wear behaviour of hardfacing ultra carbide steel grades, Surface Engineering, vol. 36, no. 11, 2020.
3. KlimpelA.: Industrial surfacing and hardfacing technology, fundamentals and applications, Welding Technology Review, vol. 91, no. 12, 2020.
4. Garbade R.R., Dhokey N.B.: Overview on Hardfacing Processes, Materials and Applications, IOP Conference Series: Materials Science and Engineering, vol. 1017, no. 1, 2021.
5. Szala M., Hejwowski T.: Cavitation erosion resistance of high-alloyed Fe-based weld hardfacings deposited via SMAW method, Tribologia, vol. 4, pp. 85–94, 2022.
6. Ivanov O., Prysyazhnyuk P., Shlapak L., Marynenko S., Bodrova L. Kramar H.: Researching of the structure and properties of FCAW hardfacing based on Fe-Ti-Mo-B-C welded under low current, Procedia Structural Integrity, vol. 36, pp. 223–230, 2022.
7. Cardoso A., Assunção E., Pires I.: Study of a hardfacing flux-cored wire for arc directed energy deposition applications, International Journal of Advanced Manufacturing Technology, vol. 118, no. 910, 2022.
8. Czupryński A.: Comparison of properties of hardfaced layers made by a metal-core-covered tubular electrode with a special chemical composition, Materials, vol. 13, no. 23, 2020.
9. SzymuraM., Czupryński A., Różański M.: Research on the properties of high chromium cast iron overlay welds deposited by tubular electrodes, Welding Technology Review, vol. 90, no. 10, 2018.
10. Pertek-Owsianna A., Wiśniewska-Mleczko K., Panfil D., Bartkowska A.: Testing the structure and properties of steels after hardfacing and laser treatment, Tribologia, vol. 2, p. 97104, 2019.
11. Kalyankar V.D., Naik H.V.: Overview of metallurgical studies on weld deposited surface by plasma transferred arc technique, Metallurgical Research and Technology, vol. 118, no. 1, 2021.
12. Czupryński A., Poloczek T., Urbańczyk M.: Characterization of a new high abrasion and erosion resistance iron-based alloy for PTA hardfacing, International Journal of Modern Manufacturing Technologies, vol. 14, no. 1, 2022.
13. Deng H., Shi H., Tsuruoka S.: Influence of coating thickness and temperature on mechanical properties of steel deposited with Co-based alloy hardfacing coating, Surface and Coatings Technology, vol. 204, no. 23, 2010.
14. Romek D., Selech J., Ulbrich D., Felusiak A., Kieruj P., Janeba-Bartoszewicz E., Pieniak D.: The impact of padding weld shape of agricultural machinery tools on their abrasive wear, Tribologia, vol. 2, pp. 5–62, 2020.
15. Thompson S.M., Bian L., Shamsaei N., Yadollahi A.: An overview of Direct Laser Deposition for additive manufacturing; Part I: Transport phenomena, modeling and diagnostics, Additive Manufacturing, vol. 8, 2015.
16. Koruba P., Jurewicz P., Reiner J., Mądry J.: Technologia ultraszybkiego napawania laserowego do nakładania powłok funkcjonalnych Stellite 6 w branży lotniczej, Przegląd Spawalnictwa, vol. 89, no. 6, p. 1519, 2017.
17. Klimpel A., Janicki D., Lisiecki A., Rzeźnikiewicz A.: Laser repair hardfacing of titanium alloy turbine Manufacturing and processing, Journal of Achievements in Materials and Manufacturing Engineering, vol. 49, no. 2, 2011.
18. Sharma S.K., Grewal H.S., Saxena K.K., Mohammed K.A., Prakash C., Davim J.P., Buddhi D., Raju R., Mohan D.G., Tomków J.: Advancements in the Additive Manufacturing of Magnesium and Aluminum Alloys through Laser-Based Approach, Materials, vol. 15, no. 22, 2022.
19. Slobodyan M.: Resistance, electron- and laser-beam welding of zirconium alloys for nuclear applications: A review, Nuclear Engineering and Technology, vol. 53, no. 4, p. 10491078, 4 2021.
20. Findik F.: Laser cladding and applications, Sustainable Engineering and Innovation, vol. 5, no. 1, 2023.

21. Wang K., Zhang Z., Xiang D., Ju J.: Research and Progress of Laser Cladding: Process, Materials and Applications, Coatings, vol. 12, no. 10, 2022.
22. Zhu L., Xue P., LanQ ., Meng G., Ren Y., Yang Z., Xu P., Liu Z.: Recent research and development status of laser cladding: A review, Optics & Laser Technology, vol. 138, p. 106915, 6 2021.
23. Adamiak M., Nana Appiah S.A., Żelazny R., Ferreira Batalha G., Czupryński A.: Experimental Comparison of Laser Cladding and Powder Plasma Transferred Arc Welding Methods for Depositing Wear-Resistant NiSiB + 60% WC Composite on a Structural-Steel Substrate, Materials, vol. 16, no. 11, 2023.
24. Singh S., Goyal D.K., Kumar P., Bansal A.: Laser cladding technique for erosive wear applications: A review, Materials Research Express, vol. 7, no. 1, 2020.
25. Bazychowska S., Starosta R., Dudzik K.: Quantitative Assessment of the Influence of Plasma Hardfacing Parameters on the Metallurgical Melting of an Austentic Steel Coating with a Substrate Material Made of C45 Steel, Journal of KONBiN, vol. 52, no. 3, p. 2751, 2022.
26. Shen Q., Xue J., Yu X., Zheng Z., Ou N.: Triple-wire plasma arc cladding of Cr-Fe-Ni-Tix high-entropy alloy coatings, Surface and Coatings Technology, vol. 443, p. 128638, 8 2022.
27. Kripalani K., Jain P.: Experimental investigations of various joinery methods on repaired AISI 304 A plate with Nitinol wire, Materials Today: Proceedings, vol. 37, no. 2, pp. 20932103, 1 2021.
28. Zhao S., Xu S., Huang Y., Yang L.: Laser hot-wire cladding of Ni/WC composite coatings with a tubular cored wire, Journal of Materials Processing Technology, vol. 298, 2021.
29. Zhao S., Xu S., Yang L., Huang Y.: WC-Fe metal-matrix composite coatings fabricated by laser wire cladding, Journal of Materials Processing Technology, vol. 301, 2022.
30. Zhao S., Yang L., Huang Y., Xu S.: A novel method to fabricate Ni/WC composite coatings by laser wire deposition: Processing characteristics, microstructural evolution and mechanical properties under different wire transfer modes, Additive Manufacturing, vol. 38, 2021.
31. Wang L., Jia C., Yuan Y., Huang Y., Yang L.: Microstructure and wear behaviors of (TiB2+TiB+TiC)/Ti coating fabricated by laser wire deposition, Materials Letters, vol. 328, p. 133132, 12 2022.
32. Torims T.: The Application of Laser Cladding to Mechanical Component Repair, Renovation and Regeneration, in DAAAM International Scientific Book, Vienna, Austria, DAAAM International, 2013, p. 587608.
33. Karip E., Aydin S., Muratoɬlu M.: A study on hardfacing alloy using Fe-Cr and Fe-B Powders, Acta Physica Polonica A, vol. 128, no. 2, 2015.
34. EN 14700:2023 – Welding consumables – Welding consumables for hard-facing, 2023.
35. EN 10025: European Standards for Structural Steel, 2019.
36. ISO 14175: Welding consumables – Gases and gas mixtures for fusion welding and allied processes, International Standards Organization, 2009.
37. ISO 6520-1 – Welding and allied processes – Classification of geometric imperfections in metallic materials – Part 1: Fusion welding, 2007.
38. ISO 9015-2 – Destructive tests on welds in metallic materials – Hardness testing – Part 2: Microhardness testing of welded joints, 2016.
39. ASTM G65 Standard Test Method for Measuring Abrasion Using the Dry Sand/Rubber Wheel Apparatus, 2018.
40. Lu Z., Rao Q., JinZ.: An investigation of the corrosion–abrasion wear behavior of 6% chromium martensitic cast steel, Journal of Materials Processing Technology, vol. 95, no. 1–3, pp. 180–184, 10 1999.
41. Li C., Li X., Yu W., Wang M., Wu R.: Effect of cooling rate on martensitic transformation initiation temperature and hardness of super high strength martensitic steel, Jinshu Rechuli/Heat Treatment of Metals, vol. 47, no. 7, 2022.
42. Greco A., Mistry K., Sista V., Eryilmaz O., Erdemir A.: Friction and wear behaviour of boron based surface treatment and nano-particle lubricant additives for wind turbine gearbox applications, Wear, vol. 271, no. 9–10, 2011.

43. Kazemipour M., Shokrollahi H., Sharafi S.: The Influence of the Matrix Microstructure on Abrasive Wear Resistance of Heat-Treated Fe-32Cr-4.5C wt% Hardfacing Alloy, Tribology Letters, vol. 39, p. 181, 2010–192.
44. Szala M., Szafran M., Matijošius J., Drozd K.: Abrasive Wear Mechanisms of S235JR, S355J2, C45, AISI 304, and Hardox 500 Steels Tested Using Garnet, Corundum and Carborundum Abrasives, Advances in Science and Technology Research Journal, vol. 17, no. 2, 2023.